Recent Change in the Connection from the Asian Monsoon to ENSO

J. L. KINTER III

Center for Ocean–Land–Atmosphere Studies, Institute of Global Environment and Society, Calverton, Maryland

K. MIYAKODA

School for Computational Sciences, George Mason University, Fairfax, Virginia

S. YANG

Climate Prediction Center, National Centers for Environmental Prediction, National Weather Service, National Oceanic and Atmospheric Administration, Camp Springs, Maryland

(Manuscript received 7 March 2001, in final form 19 October 2001)

ABSTRACT

The Asian monsoon and El Niño–Southern Oscillation (ENSO) are known to interact with each other. In this paper, four primary indices (the Indian monsoon rainfall index, the Webster and Yang monsoon index, the tropical-wide oscillation index, and the Southern Oscillation index) that characterize the temporal variation of these complex, chaotic and quasi-oscillatory phenomena are used to assess the action from the Asian monsoon to ENSO, that is, the linkage between the strong/weak monsoon and La Niña/El Niño. The evolution of the four previously documented indices and other auxiliary data over a 43-yr period is examined using the observed database and the reanalysis of the National Centers for Environmental Prediction. The Asian monsoon and ENSO intersect in a common area, namely, the warm pool in the western tropical Pacific. This region (e.g., 10°S–5°N, 110°–170°E) is located at the longitudinally central portion of the Walker circulation and also the equatorial end of the Indo-Pacific meridional overturning cell that is part of the zonal mean Hadley circulation. In recent decades, the connection between the monsoon and ENSO has changed considerably. This change is related to the atmospheric circulation over the entire North Pacific Ocean, which entered a new regime in about 1976. Before 1976, the correlations among the four primary indices, and those between the indices and the Niño-3 index of sea surface temperature, were strong. In recent decades, the ocean temperature in the entire North Pacific became considerably colder. The lower-tropospheric winds became simultaneously more cyclonic over the North Pacific. ENSO is now related to atmospheric fluctuations both in the Indian sector and in northeastern China. The western North Pacific monsoon in the vicinity of the Philippine Islands (9°–19°N, 139°–141°E) may play an important role together with the off-equatorial ocean heat content in a larger region (5°–15°N, 135°–170°E) in maintaining or even increasing ENSO activities.

1. Introduction

During the past several decades, studies have been carried out to understand the Asian monsoon and El Niño–Southern Oscillation (ENSO), the two phenomena that determine many characteristics of the short-term variability of the earth's climate. The Asian monsoon and ENSO are mutually but selectively interactive (e.g., Webster and Yang 1992), and the interaction between them is characterized by variability on decadal timescales (e.g., Kumar et al. 1999; Torrence and Webster 1999); the processes connecting the Asian monsoon to ENSO, however, especially the sequential linkage, are not fully understood. In this study, we attempt to understand the mechanisms for several important aspects of the monsoon–ENSO relationship. In particular, we focus on the physical connection through which the Asian monsoon influences ENSO. In this paper, the ''Asian monsoon'' specifically refers to the south Asian summer monsoon. We explore the features of this connection by examining different indices that measure the monsoon. We also discuss the long-term change of this connection and its relation to the broadscale climate shift. The processes through which ENSO affects the Asian monsoon are not analyzed in this study.

There have been several hypotheses on the connection of the Asian monsoon to ENSO. For example, Barnett (1983, 1984) found that propagation of anomalous atmospheric circulation features from the Indian to the Pacific sector and expansion–contraction fluctuations of the zonal overturning circulation along the equator were responsible for the coupling between the Asian monsoon

Corresponding author address: J. L. Kinter III, COLA, 4041 Powder Mill Rd., Suite 302, Calverton, MD 20705.
E-mail: kinter@cola.iges.org

© 2002 American Meteorological Society

and ENSO on interannual timescales. Rasmusson and Carpenter (1983) likewise noted a connection between the Asian monsoon and ENSO that is phase locked to the annual cycle. Yasunari (1985) pointed out the importance of surface winds over the tropical western Pacific Ocean in association with ENSO events. An important element common to each of these hypotheses is the Walker circulation (Bjerknes 1969), which straddles the Pacific and Indian Oceans along the equator. The Walker circulation is associated with the strongest large-scale atmospheric vertical motion in the world. Unlike its oceanic counterpart, the Equatorial Undercurrent, the Walker circulation is not confined near the equator, but is more changeable and chaotic. The strongest updraft is located over Indonesia and the western Pacific, where the warmest sea surface temperature (SST), the so-called warm pool, is located.

Chung and Nigam (1999) and Kirtman and Shukla (2000) investigated the hypothesis that the variability of the Asian monsoon forces ENSO, using the Zebiak and Cane (1987) coupled model and applying a parameterization of the relation between the Pacific SST (the former study) or wind stress (the latter study) and the monsoon. Both studies obtained similar results. According to Kirtman and Shukla, ''. . . monsoon variability has a profound effect on ENSO, particularly three to six months after the monsoon ends.'' On the other hand, it has been reported that the connection of the monsoon and ENSO through the Walker circulation has weakened recently (Kumar et al. 1999). More features of the change in this connection, including the related change in the large-scale background conditions in the atmosphere and oceans and their behavior as represented by different indices, will be explored in this study.

In the following section, we will introduce the indices for measuring the Asian monsoon and the datasets used in this study. The general relationship between the monsoon and ENSO will be examined in section 3. In sections 4 and 5, we will depict the processes from the monsoon to ENSO and the change in the monsoon–ENSO connection that occurred in the 1970s. Summary remarks are provided in section 6.

2. Indices and data

a. Four host indices

A common method of characterizing complex, chaotic and quasi-oscillatory phenomena is to reduce them to a single index or a small number of indices. The temporal variation of the index represents the broader phenomena and can be correlated easily with other indices. This method has been used extensively in the study of the Southern Oscillation and the Asian monsoon. For example, the Niño-3 index—the average SST in the region (5°S–5°N, 150°–90°W)—is widely used to represent El Niño/La Niña events. If a given index fits a particular phenomenon well, the associated spatial teleconnection pattern may appear as coherent and may vary regularly. The merit of using an index is to characterize the essential features of a complex phenomenon in a compact way. In particular, if the phenomenon is oscillatory, the index is effective in emphasizing some aspects of the polarity.

In this paper, four primary indices are used to explore the relationships from the Asian monsoon to ENSO. We have used multiple indices to reduce the potential bias in interpreting the results associated with using a single index. The four indices are the Indian monsoon rainfall index (IMR), the Webster and Yang index (W–Y), the tropical-wide oscillation index (TOI), and the Southern Oscillation index (SOI). The latter two indices are not designed primarily for representing the Asian monsoon, per se.

The IMR index is often called the ''All-India monsoon rainfall index'' (Mooley and Parthasarathy 1983; Parthasarathy et al. 1992). It has been used extensively, but concern recently has been expressed, because this index does not include the rainfall over the Bay of Bengal (Goswami et al. 1999; Wang and Fan 1999; Lau et al. 2000).

To represent the dynamical aspects of the Asian monsoon, we use the W–Y index, defined as the vertical shear of zonal wind (Webster and Yang 1992) between 850 and 200 hPa:

$$\text{W–Y} = U_{850} - U_{200} \tag{1}$$

averaged over the area (5°–20°N, 40°–110°E). This index has been used in many studies (e.g., Ju and Slingo 1995; Li and Yanai 1996; Lau et al. 2000) to represent the broadscale features of the Asian monsoon.

The SOI was proposed by Troup (1965) to represent the Southern Oscillation, that is, the pressure seesaw over the tropical South Pacific and the tropical Indian sector. Defined as the normalized sea level pressure anomaly difference between Darwin, Australia, and Tahiti, it has been used widely for decades to measure the ENSO phenomenon.

The TOI was proposed by Navarra et al. (1999) to represent the overall tropical circulation through the spatial distribution of precipitation. The TOI is defined as

$$\text{TOI} = \text{principal component of first EOF of precipitation} \tag{2}$$

for the domain (30°N–30°S, all longitudes), where EOF stands for empirical orthogonal function.

The IMR, W–Y, and SOI are all widely used indices of tropical phenomena in the Indian and Pacific sectors, and the TOI provides a measure of the broader-scale variability of rainfall throughout the Tropics. The four indices are the primary indicators used in this study, because we seek to identify the salient characteristics of variability in both the monsoon and the ENSO regions and also the connections between them.

b. Data sources

The data we used are monthly averages for the 43-yr period from 1955 to 1997. When a comparison is made with satellite sensor–based data, the 19 years from 1979 to 1997 (referred to as the satellite era below) are used. The principal dataset is the reanalysis of the National Centers for Environmental Prediction–National Center for Atmospheric Research (NCEP–NCAR; Kalnay et al. 1996).

The precipitation data used include the 43-yr gridded precipitation dataset over continents and islands from the University of East Anglia Climate Research Unit (Hulme 1994), and the 19-yr global NCEP Climate Prediction Center (CPC) Merged Analysis of Precipitation (known as CMAP; Xie and Arkin 1997). The SST data are from the analysis produced by the CPC (Reynolds and Smith 1994). We have compared the results based on this dataset with similar calculations made using the Global Ice and SST (GISST) analysis produced by the Hadley Centre at the Met Office (Rayner et al. 1996), and we found them to be nearly identical.

The 43-yr time series of indices, including SOI, IMR, and Niño-3, were obtained from the NCEP Web site (http://www.cpc.ncep.noaa.gov/). The Niño-3 index for NDJ(+1) was calculated from this data source, where NDJ(+1) is November and December of year 0 and January of year 1. The time series of the W–Y index was calculated from the NCEP–NCAR reanalysis.

In this paper, we also analyze the ocean heat content HC, that is,

$$\mathrm{HC} = \int_0^H T\, dz/H, \tag{3}$$

where T is the ocean temperature and H is the depth of the ocean. We use $H = 400$ m in this calculation. In exact terms, HC is the layer-mean oceanic temperature, but it is a good approximation to the heat content above 400-m depth. The gridded data of HC were computed from a model-based assimilation of expendable bathythermograph measurements of ocean temperature [described in Huang and Kinter (2001)] for the period from 1958 to 1997. The anomaly, simply denoted by HC, is the deviation from the mean of 1961–90.

The W–Y index is calculated based on the 3-month average for June–August (JJA). The SOI values are the 3-month averages for July–August–September (JAS). The IMR is calculated from the 4-month average for June–September (JJAS), and the TOI is the average for JAS. We refer to correlations among these indices and with other variables from the June–September season as nearly simultaneous correlations.

3. Monsoon–ENSO correlations

a. Correlations during 1950–97

A total of six correlations may be computed among all possible pairs chosen from the four indices (IMR, W–Y, SOI, and TOI). For the 43-yr period, a correlation coefficient larger than 0.50 is significant at the 99.9% confidence level (referred to as a strong relation), and a correlation coefficient between 0.40 and 0.49 is significant between 99.0% and 99.9% (a good relation). These critical values of correlation are based on the assumption that seasonal averages are serially uncorrelated.

TABLE 1. Correlations for the period of 1955–97. Niño-3 is the average SST in the region (5°S–5°N, 150°–90°W). Boldface numbers indicate significance above 99.9%, and italic numbers indicate significance between 99.0% and 99.9%. NDJ(+1) refers to Nov and Dec for year 0 and Jan for year 1.

Host index	Niño-3 (JAS)	Niño-3 NDJ(+1)
W–Y (JJA)	**−0.59**	*−0.42*
IMR (JJAS)	*−0.49*	**−0.50**
TOI (JAS)	**−0.87**	**−0.83**
SOI (JAS)	**−0.75**	**−0.86**

The 43-yr correlations between pairs of indices have two strong and two good relations. The TOI has two strong relations, that is, TOI versus SOI (correlation coefficient = 0.86) and TOI versus IMR (0.62), and one good relation, that is, TOI versus W–Y (0.42). Although the IMR is calculated from the local rainfall data over India and the TOI is based on the first EOF of the precipitation data over the whole tropical region, it has been found that IMR and TOI are closely related to each other. This strong correlation indicates that the variability of monsoon rainfall is an important component of the entire tropical rainfall pattern.

Table 1 shows the relation between the monsoon indices and two ENSO indices. In this study, we use Niño-3 to measure ENSO. The second column of Table 1 shows the correlation between Niño-3 for JAS and the host indices listed in the first column. The third column shows the lag correlations with SST for NDJ(+1). November–January is the peak season for El Niño/La Niña.

One of the interesting features of Table 1 is that the monsoon, measured by both W–Y and IMR, is strongly correlated with ENSO nearly simultaneously and significantly correlated with ENSO at several months lead. Although the lag correlation between W–Y and ENSO is relatively weaker, it is still significant at the 99.0% confidence level. Consistent with the concept of a ''spring predictability barrier'' (Webster and Yang 1992), the correlation in which ENSO leads the monsoon by several months is much weaker. The strong IMR–ENSO relationship when IMR leads ENSO is consistent with the findings of Shukla and Paolino (1983) and Lau and Yang (1996). In addition, Table 1 shows large coefficients for the correlations among TOI, SOI, and Niño-3, suggesting a strong coupling between the tropical atmosphere and oceans related to El Niño and La Niña events.

TABLE 2. Correlations for the period of 1979–97. The P_{sa} index is the area average of precipitation in the region 10°–30°N and 70°–100°E (Lau et al. 2000). EOF(JAS) refers to the first principal component of SST in the tropical Pacific (30°S–60°N, 120°E–80°W) based on the CPC analysis. Boldface numbers indicate correlations with significance above the 99.0% confidence level, and italic numbers have correlations significant between the 95.0 and 99.0% confidence levels.

Host index	1 P_{sa} (JJA)	2 Niño-3 (JAS)	3 EOF SST (JAS)
W–Y	0.10	*−0.54*	**−0.57**
IMR	0.41	−0.29	−0.27
TOI	0.01	**−0.82**	**−0.83**
SOI	0.05	**−0.72**	**−0.73**

b. Comparison during the satellite era

The period after 1979 is special because a proxy estimate of precipitation over the oceans is available from satellite-based observations. Table 2 shows the correlation between the host indices and precipitation and other indices for the recent 19-yr period, 1979–97. A correlation above 0.55 is significant at the 99.0% confidence level, and a correlation between 0.54 and 0.47 has a significance level between 95.0% and 99.0%.

Table 2 illustrates three different issues in the columns labeled 1–3. The column labeled 1 indicates the capability of the indices to represent the monsoon precipitation. The column labeled 2 shows the correlation coefficients with Niño-3. The column labeled 3 displays the first principal component of the EOF of the SST for the North Pacific Ocean (30°S–60°N, 120°E–80°W), whose values are similar to those calculated from the GISST (not shown).

The P_{sa} is an index of the precipitation over south Asia, that is, the area average of precipitation in the region 10°–30°N, 70°–100°E (Lau et al. 2000), in which the rainfall over the Indian subcontinent and the Bay of Bengal is included. IMR and P_{sa} have a correlation coefficient of only 0.41, suggesting that IMR is not a complete measure of the total amount of rainfall over south Asia. Note that the monsoon index proposed by Goswami et al. (1999) has a stronger correlation (0.63) with P_{sa} than with IMR (Miyakoda et al. 2000).

If the correlations of Niño-3(JAS) with various indices in Table 2 (the column labeled 2) are compared with their counterparts in Table 1 (second column), it is clear that all of the correlations in Table 2 are lower, some substantially lower. The years after 1979 are very different from the preceding years.

To examine the decrease of correlation further, pairs of variables were selected, and the correlations among these pairs were calculated using a 19-yr sliding window. Figure 1 shows the time series of correlations, computed in this way, between IMR and SOI, and between IMR and Niño-3(JAS).

According to Shukla (1995), the timing of the phase of Niño-3 and Indian summer monsoon rainfall anomalies with respect to the annual cycle is appreciably

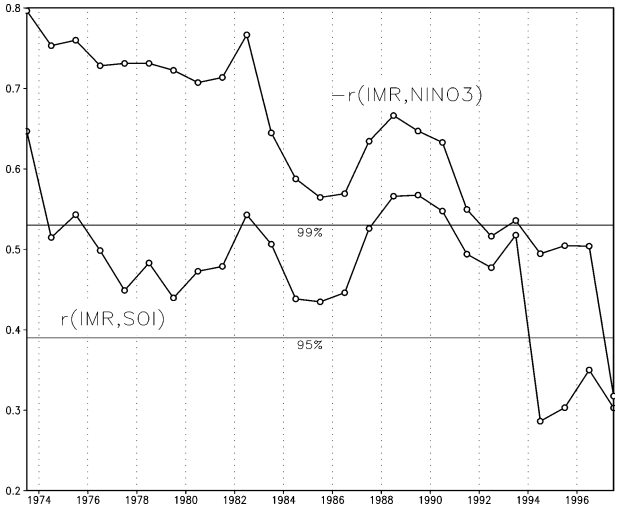

FIG. 1. Correlation coefficients for two pairs of indices, i.e., between IMR and SOI(JAS) and between −IMR and Niño-3(JAS). The correlation coefficients are shown over 19-yr sliding periods, from 1955–73 to 1979–97. The year on the abscissa indicates the last year of the window; i.e., 1974 labels the period 1956–74. Horizontal lines are included to show the 95% and 99% confidence intervals based on the Student's t statistic applied to a Fisher Z transform of the correlation (von Storch and Zwiers 1999).

different between the periods 1951–72 and 1982–91. During 1951–72, both the SST and the monsoon rainfall exhibited a biennial variation; during 1982–91, however, the SST and rainfall showed a 2-yr successive warming and a 2-yr successive decrease of precipitation, respectively. This result indicates that, although there is a close relation between ENSO and the Asian monsoon over the whole period, the time sequence of ENSO and the monsoon changes between the two periods. As a result, the interaction between the monsoon and ENSO also behaves differently, with respect to the annual cycle, between the two periods.

In summary, it has been known well that IMR is well anticorrelated (−0.49) with Niño-3(JAS), as is shown in Table 1. This strong anticorrelation has decreased to −0.29 in recent years, as shown in Table 2. Thus, in the last 20 years, there has been a significant decline in the simultaneous relation between the Asian monsoon and ENSO or the time-lagged relation from the Asian monsoon to El Niño and La Niña.

4. Processes from monsoon to ENSO

a. SST correlation patterns

The SST and the depth of the thermocline (or the ocean heat content) are the most fundamental and important oceanic indicators of the ENSO process. Figure 2 shows the correlation between the four host indices and SST in the Indian and Pacific Oceans for JJA, based on a 43-yr period. The correlation fields are characterized by the horseshoe pattern over the Pacific Ocean (Miyakoda et al. 1999). To the west, the horseshoe is

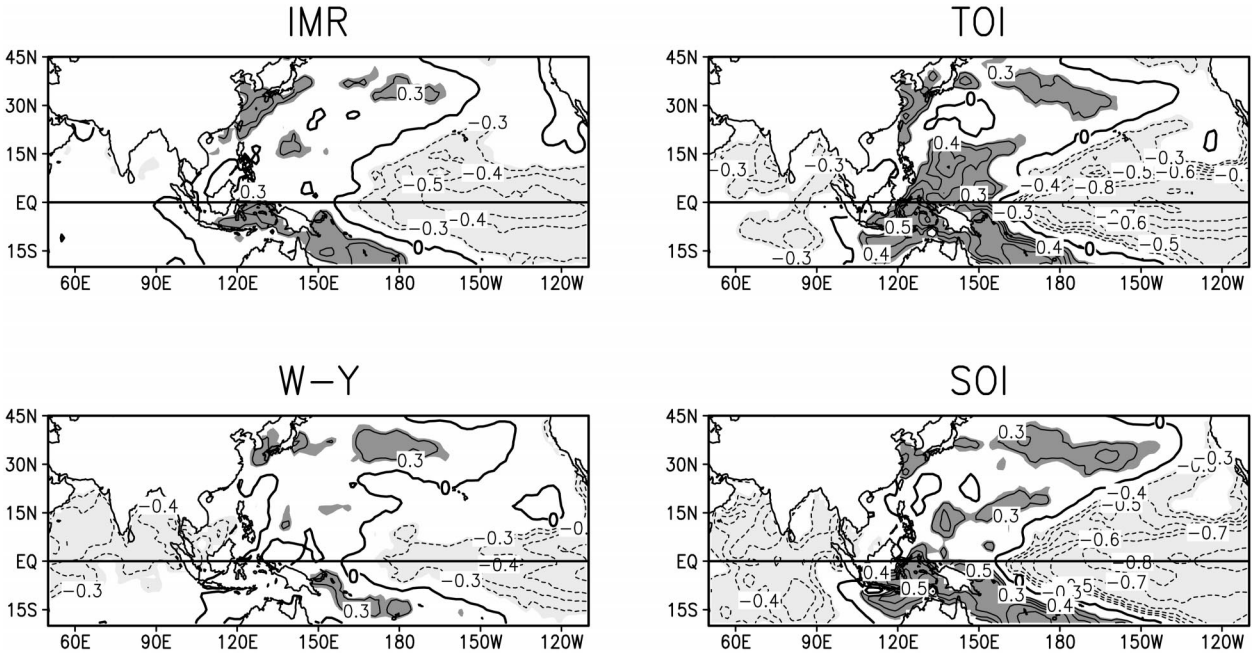

FIG. 2. Nearly simultaneous correlation patterns between the indicated host indices and SST(JJA).

surrounded by a region of opposite sign, but it is open in the vicinity of the Philippine Islands in boreal summer and appears to be connected with another correlation field over the Indian Ocean.

One interesting aspect is that the horseshoe patterns in the four panels are similar to each other. The major differences are the magnitude of the correlation and the completeness of the horseshoe shape. For NDJ(+1) or OND(0), the correlation patterns exhibit a more distinct horseshoe shape (not shown), whose correlation value is larger in the eastern Pacific and whose shape is more symmetric about the equator. The four indices may be ranked in descending order of magnitude of correlation: TOI, SOI, W–Y, and IMR. When compared with IMR and TOI, W–Y and SOI are more strongly correlated with the Indian Ocean SST (Fig. 2).

b. Atmospheric circulation patterns

Figure 3 shows the anomalous 850-hPa wind vector $\mathbf{V}_{850}$ for JJA. The figure shows the average of u_{850} and v_{850} (zonal and meridional components of $\mathbf{V}_{850}$, respectively) for the 9 largest-magnitude positive-IMR (Fig. 3a) and 9 largest-magnitude negative-IMR (Fig. 3b) years during the 43-yr period of 1955–97. In MAM (not shown), the anomalously strong Somali jet extends from Madagascar in the case of positive IMR. Then, in JJA, it branches off in two directions (Fig. 3a). One branch extends toward the Himalayas (point D), and the other extends southeastward toward Indonesia (Sumatra; point E). There simultaneously are zonal wind anomalies to the southeast of the Philippines (point F).

It is important to note that the winds at points E and D are linked together. The wind in the negative IMR composite (dry monsoon; Fig. 3b) is almost opposite to that in the positive IMR composite (Fig. 3a). The anomalous wind of the Himalayan jet (D) comes from north of India and branches off in two directions. One branch extends toward southern Indochina, and the other extends westward toward Somalia (point B), continuing to Madagascar (point A) after crossing the Indian subcontinent. The link of the wind anomalies from D to E to F can also be seen in the correlation patterns with the four primary indices (not shown).

Some portions of Figs. 3a and 3b are similar to those shown by Yang et al. (1996) and Yang and Lau (1998), based on general circulation model results obtained for several outstanding cases based on the W–Y index. The link between points E and D is also notable in their results.

5. The monsoon–ENSO relation before and after circa 1976

a. Climate shift circa 1976

Trenberth (1990) and Trenberth and Hurrell (1994) derived time series to depict changes in the Northern Hemisphere sea level pressure, including the intensity of the Aleutian low. The pressure averaged over a vast area of the North Pacific was lower by 2 hPa after 1976. Wang (1995) reported that an abrupt change occurred in the interdecadal warming in about 1977 over the tropical Pacific, concurrent with a cooling in the extratropical North and South Pacific. As a result, the sequence of El Niño evolution has changed dramatically.

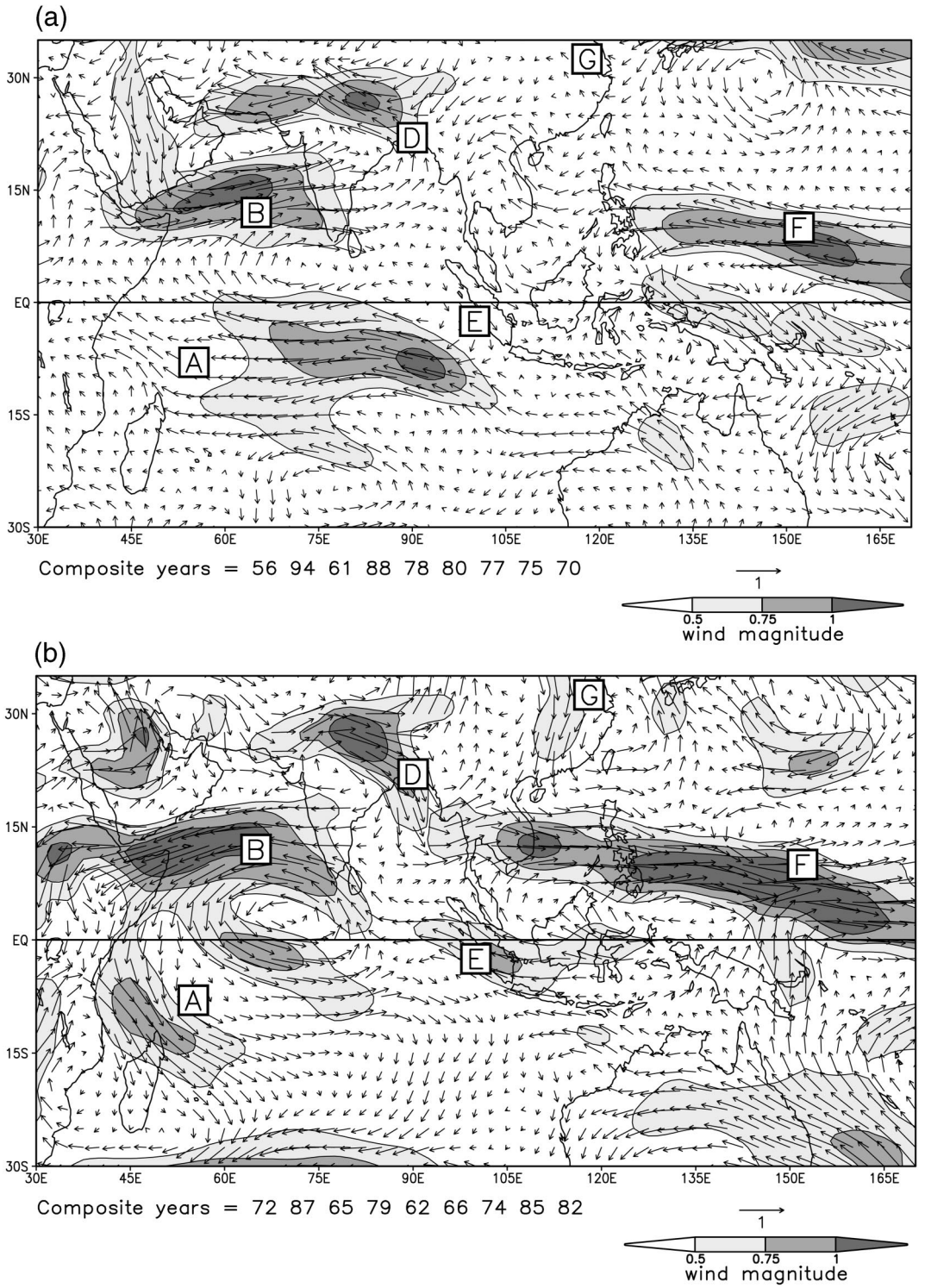

FIG. 3. (a) Anomalous 850-hPa wind for JJA. The composites are formed by averaging the nine years with largest-magnitude IMR > 0 shown at the bottom. The wind speed is indicated by shading, and the arrow scale is shown at lower right (m s^{-1}). (b) As (a) but for the case of IMR < 0. Labeled locations are discussed in text.

TABLE 3. As in Table 1 but for different base periods. The correlation coefficients are for the period of 1955–75 (left columns), and 1976–97 (right columns).

	Before 1976		After 1976	
Host index	Niño-3 (JAS)	Niño-3 NDJ(+1)	Niño-3 (JAS)	Niño-3 NDJ(+1)
W–Y	**−0.61**	**−0.59**	**−0.57**	−0.28
IMR	**−0.74**	**−0.66**	−0.25	−0.33
TOI	**−0.91**	**−0.90**	**−0.83**	**−0.78**
SOI	**−0.82**	**−0.90**	**−0.70**	**−0.82**

Later, Nakamura et al. (1997) presented a compelling argument for a 1976 climate transition based on an analysis of SST and sea level pressure over the whole Pacific Ocean. Their results indicate that the SST in the subarctic gyre region of 20°–50°N, 150°E–140°W is crucial in determining the regime shift (see also Zhang et al. 1997).

Other groups have detected this climate shift, including specialists on the fishing industry, the ecosystem, and paleoclimatology (Mantua et al. 1997; Minobe 1997). Mantua et al. reported a dramatic shift of the North Pacific marine ecosystem, that is, the salmon catch. Minobe documented the tree-ring record that is related to the continental surface temperature for three centuries. Their conclusions on the years when the climate shifted agree with each other, that is, 1925, 1947, and 1977. These two papers also emphasize the importance of nontropical components in the climate shift.

b. Index comparison between the two periods

Table 3 shows the correlations between the host indices and the indices of Niño-3 (based on the CPC SST analysis) for the periods before and after the shift, separately. All target variables have substantially reduced correlations in the second period. The decline is particularly severe for IMR, as shown for both simultaneous and lag correlations, and, second, for the lag correlation with W–Y. Also, the correlation between Niño-3 and the monsoon index proposed by Goswami et al. (1999) has decreased from 0.51 to 0.29. The variations in atmospheric and oceanic conditions associated with this change in the monsoon–ENSO relationship are discussed below.

c. Changes in the Pacific Ocean

In this section, we explore the broadscale climatic features over the Pacific Ocean that are associated with the long-term change in the monsoon–ENSO relationship. For the convenience of discussion, we will focus only on two host indices, IMR and TOI. Based on the foregoing, it is clear that IMR represents the characteristic features over the Indian sector and TOI represents the features over the Pacific sector. In connection with El Niño/La Niña, we investigate the oceanic state using SST and HC. The lower-tropospheric wind will be discussed in the section 5d.

As was described earlier, the subarctic ocean state may be involved in the climate shift. Figure 4 shows the difference in the distribution of annual mean SST before and after 1976 over the North Pacific. The SST is lower by 0.3°C in the middle of the Pacific and is higher by 0.3°C along the West Coast of North America after 1976, as compared with that before 1976, as has been shown in other studies (Douglas et al. 1982; Tanimoto et al. 1993; Miller et al. 1994). It is important to note that the patterns are not chaotic but are systematic and that the magnitude is substantial, considering the long timescale.

Yasuda and Hanawa (1997) and Deser et al. (1999)

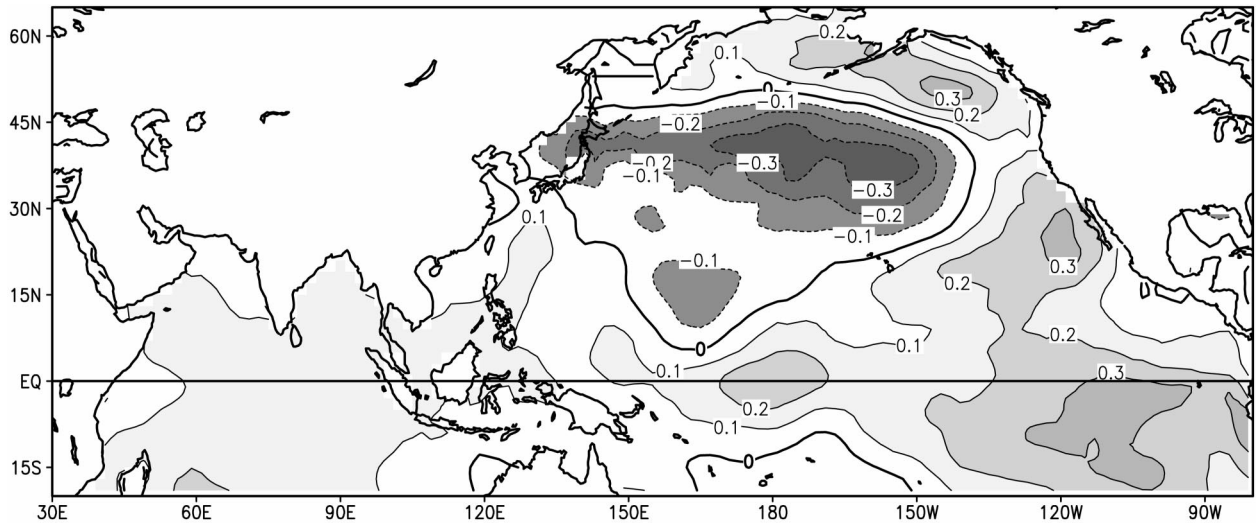

FIG. 4. SST anomaly after 1976 (°C) based on CPC analysis. The average for annual means of the 43 yr from 1955 to 1997 was subtracted from the average for the 22 yr from 1976 to 1997.

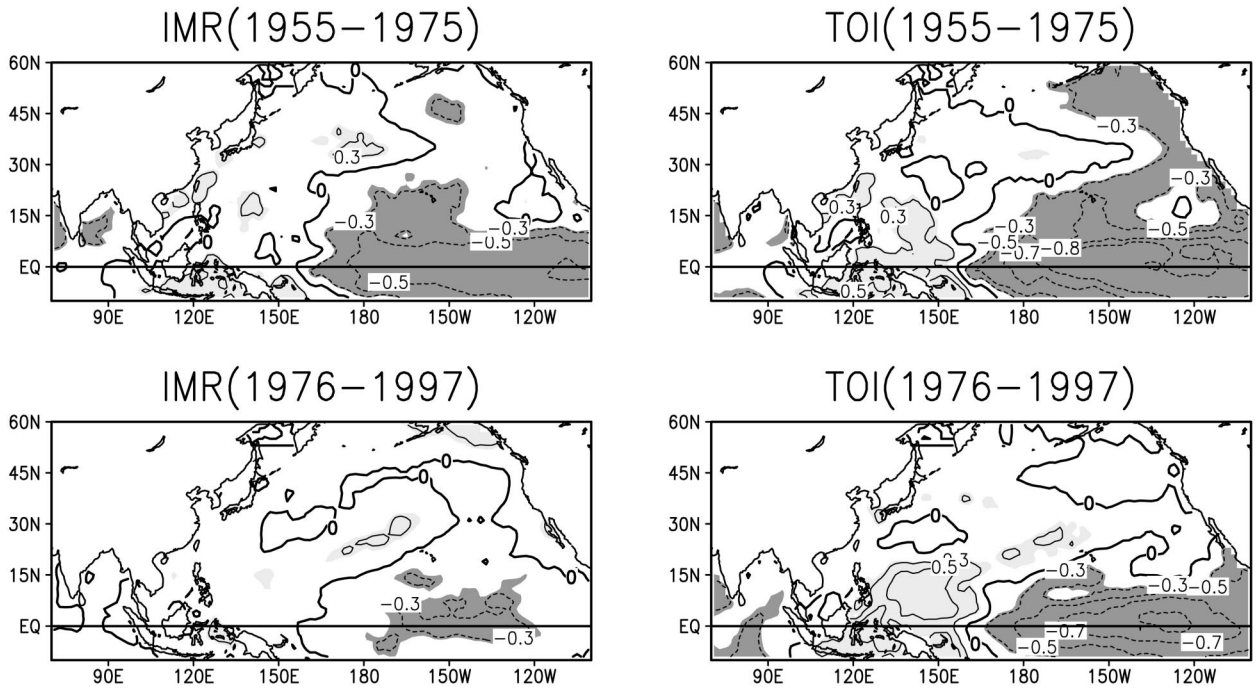

FIG. 5. Spatial distribution of correlation coefficient between the indicated host indices and SST, based on the CPC analysis, for JJA: (top) Before 1976 and (bottom) after 1976. (left) IMR is the host index, and (right) TOI is the host index.

showed that there was a substantial temperature change of the North Pacific mode water over the Kuroshio extension down to 400–500-m depth. Numerical simulation experiments by Deser et al. (1999) and Xie et al. (2000) indicate that the consistently strong westerlies over northern Japan and the eastward extension of the Kuroshio Current are primarily responsible for creating the cold water.

Figure 5 shows the simultaneous correlation between TOI and SST, and between IMR and SST, both for JJA. These figures are similar to those shown in Fig. 2 but are divided into the two epochs and are expanded to include the subarctic region in the Northern Hemisphere. After 1976, the ENSO effect is still clear in the case of TOI, but it is very weak in the case of IMR. The contrast of the correlation patterns with IMR before and after 1976 is striking. This result confirms that the Indian summer monsoon rainfall (IMR) has a weaker relation with the subsequent ENSO after 1976 (correlation coefficient 0.25–0.33) than before 1976 (correlation coefficient 0.66–0.74), as indicated in Table 3.

The mechanism for ENSO events has been explained with the ''delayed oscillator'' concept (Suarez and Schopf 1988; Battisti and Hirst 1989). Consistent with this concept, there is a systematic development of the distribution of the anomalous HC(JJA) associated with El Niño and La Niña events, particularly in the western Pacific Ocean. Six months prior to the initiation of the ENSO, the positive-HC-anomaly lobes (Geise and Carton 1999) emerge in the western Pacific (120°–170°E), first between 5° and 10°N and subsequently (4 months prior to the initiation in the eastern Pacific) in the equatorial zone (5°N–5°S). Note that the correlation between the two indices and HC(JJA) indicates different behavior before and after 1976 in the case of IMR but similar behavior in the two periods in the case of TOI (see Miyakoda et al. 2000).

d. Changes in atmospheric circulation

To understand the change in SST after 1976 better, the lower-tropospheric wind over the western tropical Pacific, one of the crucial factors relating to subsequent ENSO events, was examined. The change of $\mathbf{V}_{850}$ after 1976 is so dramatic that simply taking the difference between the two periods clearly shows the change. Figure 6 is the vector difference in annual mean $\mathbf{V}_{850}$ before and after 1976. The most notable features in the Asian–Pacific sector are (i) the anomalous cyclonic circulation over the North Pacific centered at 165°W and 50°N [point a; similar to Deser et al. (1999), see their Fig. 1]; (ii) the westerlies (point F) at 150°–120°W and 10°N; (iii) the increased northerly flow over eastern China (G) associated with the broadscale wind change that is one of the largest-amplitude changes over the globe; and (iv) the small cells of anomalous cyclonic and anticyclonic flow that are aligned side by side (see next section) to the east of the Philippine Islands. The cyclonic pattern, or the weakened anticyclonic pattern, over the subtropical western Pacific is consistent with the weakening of the relationship between the monsoon and ENSO.

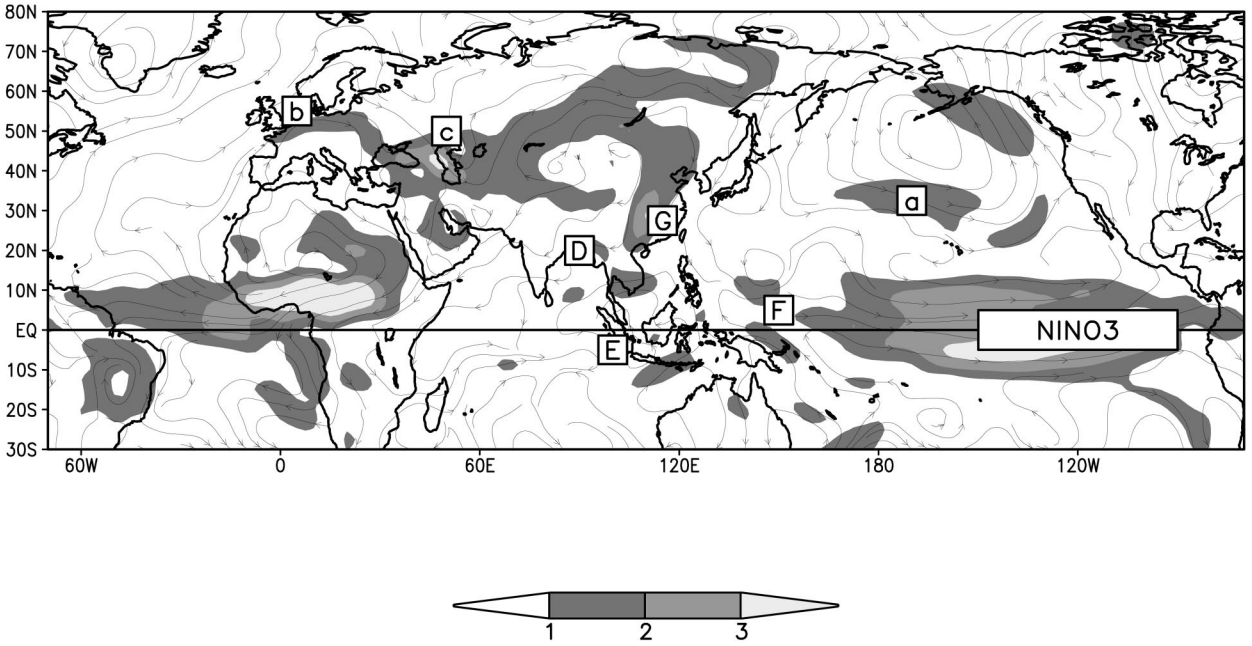

FIG. 6. Difference in annual-mean 850-hPa wind vectors, 1976–98 average minus 1958–75 average. Wind direction is indicated by streamlines, and the speed is shown with shading (scale at bottom; m s^{-1}). Points D, E, F, and G and the box Niño-3 are related to the Asian monsoon and ENSO, and points a, b, and c are related to Eurasian and Pacific phenomena.

The most outstanding difference in the flow is near the point G (see also Fig. 3). The flow at G may be considered as the local manifestation of the zonal mean Hadley circulation in the Asian sector. The anomaly of this flow is in the opposite direction before and after 1976.

e. Other aspects of the monsoon–ENSO relationship after 1976

Here, we further describe the monsoon–ENSO relationship during the recent decades, after 1976. From the previous analysis, we have noticed other outstanding features in the Asian monsoon region that are linked to ENSO, for example, the zonal wind u_{850} at point F and the meridional wind v_{850} at point G in Fig. 6. To understand these features better, the construction of additional indices is helpful. We define two indices: U_{ph} (u_{850} near the Philippine Islands averaged over 0°–10°N, 140°–160°E) and V_{ch} (v_{850} over northeast China averaged over 20°–35°N, 110°–120°E), both for JAS (Fig. 7). According to Li (1990), V_{ch} is an index for measuring the east Asian winter monsoon, which the author claimed to be an important mechanism in El Niño. Lu and Chan (1999) selected the meridional wind at 1000 hPa averaged over the domain 7.5°–20°N, 107.5°–120°E for JJA as the ''unified monsoon index'' for south China. This unified index is very similar to V_{ch}; the only differences are the wind level (1000 vs 850 hPa) and the domain (7.5°–20°N vs 20°–35°N).

We also define the HC index (HCI) as the time series of HC averaged over the off-equatorial domain (5°–15°N, 135°–170°E) for JAS (Fig. 7). In fact, the area of HCI overlaps with the area sampled by a Japanese research vessel (2°–10°N, 137°E), the data of which were used by Yasunari (1990) for advocating the relationship between IMR and the oceanic mixed-layer temperature in that area. HCI is correlated well with Niño-3 both before and after 1976, and the use of HCI is essential in the explanation of the ENSO process for the latter period, as described below.

By using satellite-based observational data, the monsoon centers in the tropical and subtropical Pacific can be identified more clearly, as compared with the analysis of observations from the presatellite era. One of the examples is the western North Pacific monsoon (WNPM) defined by Murakami and Matsumoto (1994), over the area 5°–20°N and 120°–160°E (Fig. 7). This monsoon is associated with the cyclonic cell east-northeast of the Philippine Islands. We computed the WNPM(Jul) from the July average anomalous mean sea level pressure of the NCEP–NCAR reanalysis as the difference between a northern (19°–21°N, 139°–141°E) and a southern (9°–11°N, 139°–141°E) area (see Fig. 7). This is similar to Tanaka's (1997) definition that used the 20–29 July mean and the difference between 10° and 20°N.

Table 4 gives the correlation coefficient among the different host indices. We chose Niño-3(JJA), U_{ph}(JJA), and WNPM(Jul) because the first two are fundamental variables associated with ENSO and because WNPM is relevant to the 1976 transition. There are three groups

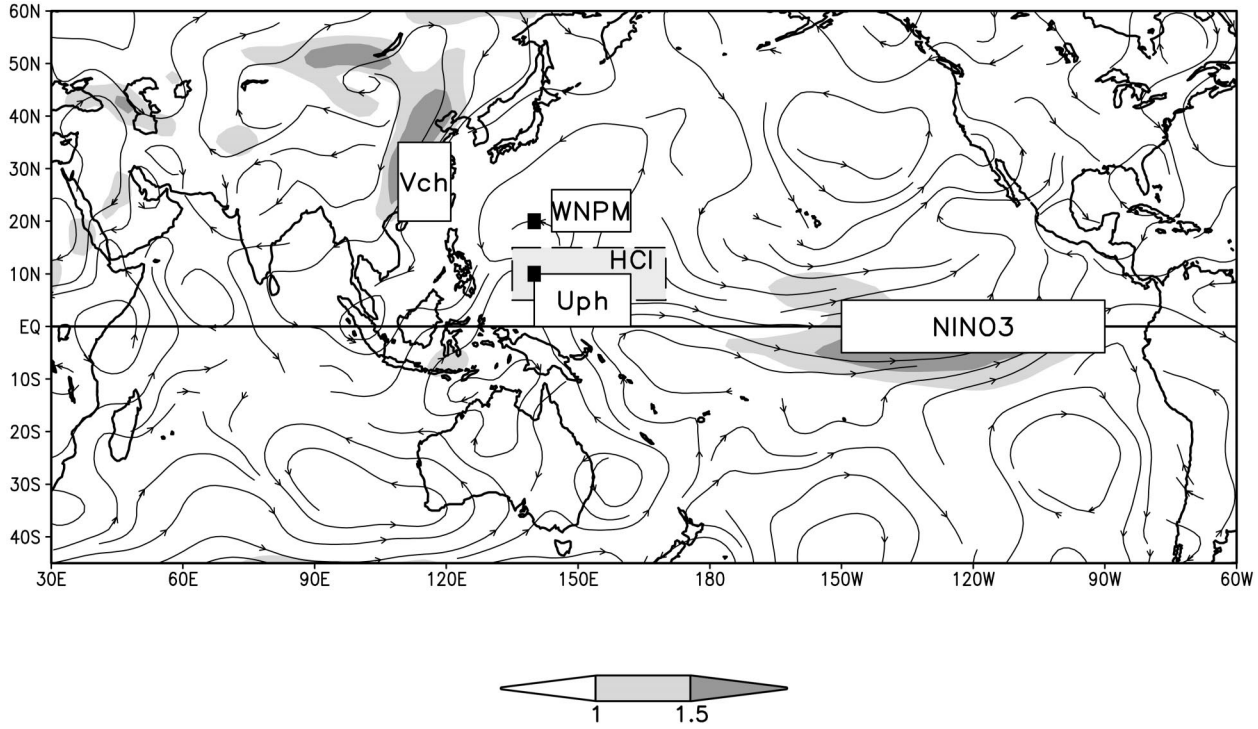

FIG. 7. Explanation of Table 4. Shown are streamlines of 850-hPa wind anomalies for JJA after 1976. The intensity of wind is shown at the bottom (m s^{-1}). The boxes labeled V_{ch}, WNPM, HCI, U_{ph}, and Niño-3 are the regions of area averaging for the indicated indices. Small filled boxes indicated locations at which the difference is computed for the WNPM.

as indicated in Table 4, that is, A, B, and C. Group A includes the primary four host indices. Group B includes the intermediate ENSO variables, as opposed to the basic ENSO indices. Group C includes the new members, which are unique after 1976.

The correlations in group A indicate the degrees of connection between ENSO and the four primary indices. As has been seen previously, the correlations of the four indices in group A with Niño-3 and U_{ph} are reduced after 1976, especially that between IMR and Niño-3. However, the correlations with WNPM are uniquely high in the later period. The correlation between W–Y and WNPM and that between TOI and WNPM are high only after 1976. This result may be because W–Y has some connection with the northern part of Southeast Asia (Lau et al. 2000) and because the TOI tends to be more heavily weighted over the western Pacific.

The U_{ph} index and HCI in group B are important indicators of the ENSO delayed oscillator. Group B may be summarized as follows: (i) The U_{ph} index has had a

TABLE 4. Correlation coefficients among the possibly relevant variables and indices for the ENSO before and after 1976. Symbol U_{ph} is the area average of u_{850} (0°–10°N, 140°–160°E). WNPM is the western North Pacific monsoon index defined as the difference in sea level pressure between the two domains (19°–21°N, 139°–141°E) and (9°–11°N, 139°–141°E). Symbol W–Y is the Webster and Yang index (Webster and Yang 1992). IMR is the all-India monsoon rainfall index (Mooley and Partharsarthy 1983). TOI is the tropical-wide oscillation index (Navarra et al. 1999). SOI is the Southern Oscillation index (Troup 1965). HCI is the area average (5°–15°N, 135°–170°E) of the oceanic layer-mean temperature (0–400-m depth). Symbol V_{ch} is the area average of v_{850} (20°–35°N, 110°–120°E). Boldface numbers indicate significance greater than 99.0%; italic numbers indicate significance between 80.0% and 99.0%.

		Before 1976			After 1976		
	Host index	Niño-3 SST(JAS)	U_{ph} (JJA)	WNPM (Jul)	Niño-3 SST(JAS)	U_{ph} (JJA)	WNPM (Jul)
A	W–Y	**−0.61**	*−0.50*	0.16	**−0.57**	*−0.40*	*−0.45*
	IMR	**−0.74**	**−0.66**	0.14	−0.25	*−0.50*	−0.25
	TOI	**−0.91**	**−0.92**	0.06	**−0.83**	**−0.82**	**−0.56**
	SOI	**−0.82**	**−0.88**	−0.02	**−0.70**	**−0.80**	−0.18
B	U_{ph}	**0.91**	—	−0.12	**0.80**	—	0.25
	HCI	**−0.70**	**−0.72**	0.03	**−0.64**	**−0.60**	*−0.43*
C	WNPM	−0.02	−0.12	—	*−0.51*	0.25	—
	V_{ch}	−0.16	−0.12	**−0.48**	**−0.55**	*−0.42*	*−0.39*

very high correlation with Niño-3 for the 43-yr period of this study. As was pointed out by Luther et al. (1983) and Harrison and Giese (1991), the westerly wind bursts over the western tropical Pacific are crucial for triggering the warming of the tropical Pacific. Harrison and Vecchi (1997) studied the spatial and temporal characteristics of the westerly wind events over the western tropical Pacific for the period of 1986–95. The area near point F is included as a part (52%) of the whole area they studied. (ii) The correlations between HCI(JAS) and Niño-3(JAS) are −0.70 and −0.64 before and after 1976, respectively. The HCI signal precedes Niño-3, suggesting that HCI is a precursor for El Niño/La Niña.

In group C, significant correlations are found after 1976. The only exception is the strong relation between V_{ch} and WNPM (correlation −0.48) before 1976. The reason for this relation is unclear. A crucial point is that V_{ch}(JAS) or WNPM contributes to Niño-3 SST only after 1976 (−0.51 and −0.55, respectively).

After 1976, the Asian monsoon rainfall is not a good indicator of the activity of ENSO, but the connections from the monsoon east-northeast of the Philippine Islands (WNPM) to ENSO and from the northeast China monsoon (V_{ch}) to ENSO have increased. It is admitted that the value of correlation is not very high. It is worth noting that HCI has significant correlations with Niño-3 (−0.70 and −0.64) before and after 1976, respectively.

6. Summary and discussion

a. Summary

The connection from the Asian monsoon to ENSO was examined using four primary indices (IMR, W–Y, SOI, and TOI) and several auxiliary indices for the 43-yr period from 1955 to 1997. The data used for this study are mainly the NCEP–NCAR reanalysis and a model-based ocean data assimilation. Depending upon the periods, that is, before or after the mid-1970s, the features associated with the connection from the monsoon to ENSO are different.

Before 1976, the correlation coefficients among the four main indices are very high. The correlation coefficients between each of the four primary indices and Niño-3 as well as the principal component of the first EOF of North Pacific SST are also strong. In other words, the Asian monsoon was a precursor for ENSO.

After 1976, however, the correlation coefficients among some indices become considerably lower, and the lag-correlation coefficients with Niño-3 also substantially decreased except in the cases of TOI and SOI. Thus, the Asian monsoon has not been a good precursor for ENSO in recent years.

Circa 1976, the SST over the extratropical North Pacific cooled by about 0.3°C. Associated with this change of the underlying ocean temperature is a broadscale cyclonic wind anomaly in the lower troposphere (e.g., at 850 hPa). In correspondence, both the northerly flow V_{ch} over northeast China and the western North Pacific monsoon over the area east of the Philippine Islands clearly became more important. This development is shown in Table 4 by the fact that WNPM and V_{ch} are significantly more strongly anticorrelated with Niño-3 after 1976 than before 1976. Over the same period, V_{ch} has become significantly more strongly anticorrelated with U_{ph} while U_{ph} has become significantly less anticorrelated with the Asian monsoon indices IMR and W–Y.

The above changes in correlation can be interpreted as follows. Before 1976, ENSO was uniquely and closely related to atmospheric circulation and precipitation in the Indian sector; after 1976, ENSO was related both to the atmospheric circulation over northeastern China and to the Indian sector. Both before and after 1976, the connection from the Asian monsoon to ENSO is accomplished by affecting first the heat content in the western off-equatorial Pacific and then the westerlies over the western equatorial Pacific.

b. Discussion

The weakening of the relationship between the Asian monsoon and ENSO has been described in a number of previous studies (e.g., Kumar et al. 1999; Torrence and Webster 1999; Krishnamurthy and Goswami 2000; Chang et al. 2001). In particular, Krishnamurthy and Goswami investigated the relation between IMR and Niño-3 for the 126-yr period from 1871 to 1995. Using an 11-yr sliding-window correlation, the authors found a climate shift that may affect the monsoon–ENSO connection after 1976, similar to the result shown in this paper. Evidence related to the climate shift has been reported in the changes of eastern equatorial Pacific SST (Elliott and Angell 1988; Gu and Philander 1995), the magnitude of ENSO and monsoon anomalies (Torrence and Webster 1999), and atmospheric jet streams (Chang et al. 2001). All relevant studies, including our current study, face several difficulties in understanding this change in the monsoon–ENSO relationship. First, there is uncertainty in the long-term variations in the data, including the trend, due to fluctuations in the data quality. Second, a problem that is common to all the studies of monsoon on various timescales exists in the representation of the monsoon by different data fields and geographical domains. It is possible that the difference in monsoon anomalies resulting from the different definitions of the monsoon can be larger than the monsoon variability measured by a specific index. Third, there are many possible physical mechanisms for the weakening in the monsoon–ENSO relationship. There may be decadal variations in the monsoon or in ENSO separately, the Indo-Pacific tropical region may experience a coupled ocean–atmosphere oscillation on decadal timescales, or there may be a remote decadal variation that influences one or both of these phenomena. As an example of the last possibility, Chang et al. (2001) suggested that the strengthening and poleward shift of the

upper-tropospheric jet over the North Atlantic, associated with the North Atlantic Oscillation, may influence the monsoon on decadal timescales through its effect on Eurasian surface temperature.

In this study, we have linked the weakening in the monsoon–ENSO relationship to the change in North Pacific SST and the associated change in the overlying atmospheric circulation, especially that over east Asia and the western Pacific. It is possible that the intensification of the atmospheric cyclonic flow over the North Pacific after 1976 (see Fig. 6) is linked to the North Atlantic Oscillation, which yields a certain consistency with the result of Chang et al. (2001). We have investigated the change (before and after 1976) by exploring the lag relationship associated with the processes from the Asian monsoon to ENSO, which may aid understanding of the weakening in the monsoon–ENSO relationship. Although our lag-correlation analysis cannot establish a cause-and-effect relationship, we believe further study of these regional phenomena is warranted.

Acknowledgments. The authors are grateful to Prof. J. Shukla and Dr. Kenneth Mooney for their encouragement. We thank Dr. Bohua Huang for providing the ODA dataset and Mr. Brian Doty for providing assistance with GrADS. Suggestions provided by two anonymous reviewers substantially improved the manuscript, and their recommendations are gratefully acknowledged. This research was supported, in part, by NOAA under Grant NA96-GP0389 and, in part, by NSF, NOAA, and NASA under Grants ATM-9814295, NA96GP0056, and NAG5-8202, respectively.

REFERENCES

Barnett, T. P., 1983: Interaction of the monsoon and Pacific trade wind systems at interannual time scales. Part I: The equatorial zone. *Mon. Wea. Rev.,* **111,** 756–773.

——, 1984: Interaction of the monsoon and Pacific trade wind system at interannual time scales. Part III: A partial anatomy of the Southern Oscillation. *Mon. Wea. Rev.,* **112,** 2388–2400.

Battisti, D. S., and A. C. Hirst, 1989: Interannual variability in the tropical atmosphere–ocean model: Influence of the basic state, ocean geometry, and nonlinearity. *J. Atmos. Sci.,* **46,** 1687–1712.

Bjerknes, J., 1969: Atmosphere teleconnections from the equatorial Pacific. *Mon. Wea. Rev.,* **97,** 163–172.

Chang, C.-P., P. Harr, and J. Ju, 2001: Possible roles of Atlantic circulations on the weakening Indian monsoon rainfall–ENSO relationship. *J. Climate,* **14,** 2376–2380.

Chung, C., and S. Nigam, 1999: Asian summer monsoon–ENSO feedback on the Cane–Zebiak model ENSO. *J. Climate,* **12,** 2787–2807.

Deser, C., M. A. Alexander, and M. S. Timin, 1999: Evidence for a wind-driven intensification of the Kuroshio Current extension from the 1970s to the 1980s. *J. Climate,* **12,** 1697–1706.

Douglas, A. V., D. R. Cayan, and J. Namias, 1982: Large-scale changes in North Pacific and North American weather patterns in recent decades. *Mon. Wea. Rev.,* **110,** 1851–1862.

Elliott, W. P., and J. K. Angell, 1988: Evidence for changes in Southern Oscillation relationships during the last 100 years. *J. Climate,* **1,** 729–737.

Giese, B. S., and J. A. Carton, 1999: Interannual and decadal variability in the tropical and midlatitude Pacific Ocean. *J. Climate,* **12,** 3402–3418.

Goswami, B. N., V. Krishnamurthy, and H. Annamalai, 1999: A broad scale circulation index for interannual variability of the Indian summer monsoon. *Quart. J. Roy. Meteor. Soc.,* **125,** 611–633.

Gu, D., and S. G. H. Philander, 1995: Secular changes of annual and interannual variability in the Tropics during the past century. *J. Climate,* **8,** 864–876.

Harrison, D. E., and B. S. Giese, 1991: Episodes of surface westerly winds as observed from islands in the western tropical Pacific. *J. Geophys. Res.,* **96,** 3221–3237.

——, and G. A. Vecchi, 1997: Westerly wind events in the tropical Pacific, 1986–95. *J. Climate,* **10,** 3131–3156.

Huang, B., and J. L. Kinter III, 2001: The interannual variability in the tropical Indian Ocean and its relations to El Niño/Southern Oscillation. COLA Tech. Rep. 94, 48 pp. [Available from COLA, 4041 Powder Mill Road, Suite 302, Calverton, MD 20705.]

Hulme, M., 1994: Validation of large-scale precipitation fields in general circulation models. *Global Precipitation and Climate Change,* M. Desbois and F. Desalmans, Eds., NATO ASI Series I, Vol. 26, Springer-Verlag, 387–406.

Ju, J., and J. M. Slingo, 1995: The Asian summer monsoon and ENSO. *Quart. J. Roy. Meteor. Soc.,* **121,** 1133–1168.

Kalnay, E., and Coauthors, 1996: The NCEP/NCAR 40-Year Reanalysis Project. *Bull. Amer. Meteor. Soc.,* **77,** 437–471.

Kirtman, B. P., and J. Shukla, 2000: Influence of the Indian summer monsoon on ENSO. *Quart. J. Roy. Meteor. Soc.,* **126,** 1–27.

Krishnamurthy, V., and B. N. Goswami, 2000: Indian monsoon–ENSO relationship on interdecadal timescale. *J. Climate,* **13,** 579–595.

Kumar, K. K., B. Rajagopalan, and M. A. Cane, 1999: On the weakening relationship between the Indian monsoon and ENSO. *Science,* **284,** 2156–2159.

Lau, K.-M., and S. Yang, 1996: The Asian monsoon and predictability of the tropical ocean–atmosphere system. *Quart. J. Roy. Meteor. Soc.,* **122,** 945–957.

——, K.-M. Kim, and S. Yang, 2000: Dynamical and boundary forcing characteristics of regional components of the Asian summer monsoon. *J. Climate,* **13,** 2461–2482.

Li, C., 1990: Interaction between anomalous winter monsoon in East Asia and El Niño events. *Adv. Atmos. Sci.,* **7,** 36–46.

——, and M. Yanai, 1996: The onset and interannual variability of the Asian monsoon in relation to land–sea thermal contrast. *J. Climate,* **9,** 358–375.

Lu, E., and J. C. L. Chan, 1999: A unified monsoon index for South China. *J. Climate,* **12,** 2375–2385.

Luther, D. S., D. E. Harrison, and R. A. Knox, 1983: Zonal winds in the central equatorial Pacific and El Niño. *Science,* **222,** 327–330.

Mantua, J. N., S. R. Hare, Y. Zhang, J. M. Wallace, and R. C. Francis, 1997: A Pacific interdecadal climate oscillation with impacts on salmon production. *Bull. Amer. Meteor. Soc.,* **78,** 1069–1080.

Miller, A. J., D. R. Cayan, T. P. Barnett, N. E. Graham, and J. M. Oberhuber, 1994: Interdecadal variability of the Pacific Ocean model response to observed heat flux and wind stress anomalies. *Climate Dyn.,* **9,** 287–302.

Minobe, S., 1997: A 50–70 year climatic oscillation over the North Pacific and North America. *Geophys. Res. Lett.,* **24,** 683–686.

Miyakoda, K., A. Navarra, and M. N. Ward, 1999: Tropical-wide teleconnection and oscillation. II: The ENSO–monsoon system. *Quart. J. Roy. Meteor. Soc.,* **125,** 2937–2963.

——, J. Kinter, and S. Yang, 2000: Analysis of the connection from the South Asian monsoon to ENSO by using precipitation and circulation indices. COLA Tech. Rep. 90, 72 pp. [Available from COLA, 4041 Powder Mill Rd., Suite 302, Calverton, MD 20705.]

Mooley, D. A., and B. Parthasarathy, 1983: Variability of the Indian summer monsoon and tropical circulation features. *Mon. Wea. Rev.,* **111,** 967–978.

Murakami, T., and J. Matsumoto, 1994: Summer monsoon over the

Asian continent and western North Pacific. *J. Meteor. Soc. Japan,* **72,** 719–745.
Nakamura, H., G. Lin, and T. Yamagata, 1997: Decadal climate variability in the North Pacific during the recent decades. *Bull. Amer. Meteor. Soc.,* **78,** 2215–2225.
Navarra, A., M. N. Ward, and K. Miyakoda, 1999: Tropical-wide teleconnection and oscillation. I: Teleconnection indices and type I/type II states. *Quart. J. Roy. Meteor. Soc.,* **125,** 2909–2935.
Parthasarathy, B., R. R. Kumar, and D. R. Kothawale, 1992: Indian summer monsoon rainfall indices, 1871–1990. *Meteor. Mag.,* **121,** 174–186.
Rasmusson, E. M., and T. H. Carpenter, 1983: The relationship between eastern equatorial Pacific sea surface temperatures and rainfall over India and Sri Lanka. *Mon. Wea. Rev.,* **111,** 517–528.
Rayner, N. A., E. B. Horton, D. E. Parker, C. K. Folland, and R. B. Hackkett, 1996: Version 2.2 of the global sea-ice and sea surface temperature data set, 1903–1994. Hadley Centre for Climate Prediction and Research Climate Res. Tech. Note 74, 35 pp.
Reynolds, R. W., and T. M. Smith, 1994: Improved global sea surface temperature analysis using optimum interpolation. *J. Climate,* **7,** 929–948.
Shukla, J., 1995: Predictability of the tropical atmosphere, the tropical oceans and TOGA. *Proc. Int. Conf. on the Tropical Ocean and Global Atmosphere (TOGA)Programme,* 2, WCRP-91, World Climate Research Programme, Geneva, Switzerland, 725–730.
——, and D. A. Paolino, 1983: The Southern Oscillation and long range forecasting of the summer monsoon rainfall over India. *Mon. Wea. Rev.,* **111,** 1830–1837.
Suarez, M. J., and P. S. Schopf, 1988: A delayed oscillator for ENSO. *J. Atmos. Sci.,* **45,** 3283–3287.
Tanaka, M., 1997: Interannual and interdecadal variations of the western North Pacific monsoon and Baiu rainfall and their relationship to the ENSO cycles. *J. Meteor. Soc. Japan,* **75,** 1109–1123.
Tanimoto, Y., N. Iwasaka, K. Hanawa, and Y. Toba, 1993: Characteristic variations of sea surface temperature with multiple time scales in the North Pacific. *J. Climate,* **6,** 1153–1160.
Torrence, C., and P. J. Webster, 1999: Interdecadal changes in the ENSO–monsoon system. *J. Climate,* **12,** 2679–2690.
Trenberth, K. E., 1990: Recent observed interdecadal climate changes in the Northern Hemisphere. *Bull. Amer. Meteor. Soc.,* **71,** 988–993.
——, and J. W. Hurrell, 1994: Decadal atmosphere–ocean variations in the Pacific. *Climate Dyn.,* **9,** 303–319.
Troup, A. J., 1965: The Southern Oscillation. *Quart. J. Roy. Meteor. Soc.,* **91,** 490–506.
von Storch, H., and F. Zwiers, 1990: *Statistical Analysis in Climate Research.* Cambridge University Press, 484 pp.
Wang, B., 1995: Interdecadal changes in EL Niño onset in the last four decades. *J. Climate,* **8,** 267–285.
——, and Z. Fan, 1999: Choice of South Asian summer monsoon indices. *Bull. Amer. Meteor. Soc.,* **80,** 629–638.
Webster, P. S., and S. Yang, 1992: Monsoon and ENSO: Selectively interactive systems. *Quart. J. Roy. Meteor. Soc.,* **118,** 877–926.
Xie, P., and P. A. Arkin, 1997: Global precipitation: A 17-year monthly analysis based on gauge observations, satellite estimates and numerical model outputs. *Bull. Amer. Meteor. Soc.,* **78,** 2539–2558.
Xie, S.-P., T. Kunitani, and A. Kubokawa, 2000: Interdecadal thermocline variability in the North Pacific for 1958–97: A GCM simulation. *J. Phys. Oceanogr.,* **30,** 2798–2813.
Yang, S., and K.-M. Lau, 1998: Influences of sea surface temperature and ground wetness on Asian summer monsoon. *J. Climate,* **11,** 3230–3246.
——, ——, and M. Sankar-Rao, 1996: Precursory signals associated with the interannual variability of the Asian summer monsoon. *J. Climate,* **9,** 949–964.
Yasuda, T., and K. Hanawa, 1997: Decadal changes in the mode waters in the midlatitude North Pacific. *J. Phys. Oceanogr.,* **27,** 858–870.
Yasunari, T., 1985: Zonally propagating modes of the global east–west circulation associated with the Southern Oscillation. *J. Meteor. Soc. Japan,* **63,** 1013–1029.
——, 1990: Impact of Indian monsoon on the coupled atmosphere/ocean system in the tropical Pacific. *Meteor. Atmos. Phys.,* **44,** 29–41.
Zebiak, S. E., and M. A. Cane, 1987: A model of El Niño and the Southern Oscillation. *Mon. Wea. Rev.,* **115,** 2262–2278.
Zhang, Y., J. M. Wallace, and D. S. Battisti, 1997: ENSO-like interdecadal variability: 1990–93. *J. Climate,* **10,** 1004–1020.